抑制し，分化抑制・増殖促進の状態を保つ。その後，胚中心細胞の成熟化にむけて EZH2 の発現量は減少し，細胞分化が進捗する。一方，この過程において EZH2 の制御が外れて H3K27me3 が恒常的に高レベルになると，分化関連因子や細胞周期阻害因子の抑制が継続され，FL や GCB 型 DLBCL 等の B 細胞性リンパ腫発症の一因となると考えられる（Beguelin, et al., 2013; Caganova, et al., 2013; Beguelin, et al., 2016）（図 2.6.2.6-1）。FL は，がん化した胚中心芽細胞と胚中心細胞が濾胞状の形態を保ったまま増殖する組織像を呈し，病症が比較的緩慢に進行するインドレントリンパ腫である。一方，GCB 型 DLBCL では，がん化した胚中心芽細胞と胚中心細胞が濾胞構造をはみ出し，リンパ組織全体にびまん性に増殖する組織像を呈し，病症経過の速いアグレッシブリンパ腫である。

FL や GCB 型 DLBCL では EZH2 の SET ドメイン領域での遺伝子変異（A682G，A692V，Y646F，Y646C，Y646H，Y646N，Y646S 等*）が報告されており，EZH2 活性の亢進により高レベルの H3K27me3 が生成されて，変異型 EZH2 に依存した腫瘍増殖をおこす（Morin, et al., 2010; Sneeringer, et al., 2010; Yap, et al., 2011; Bödör, et al., 2013）。最近，変異型 EZH2 は組織適合性抗原クラス I とクラス II の発現を抑制し，宿主からの免疫攻撃を回避することによって腫瘍を悪性化するということも報告されている（Ennishi, et al., 2019）。したがって，タゼメトスタット等 EZH2 阻害剤は，FL や GCB 型 DLBCL 等に対する有力な治療法を提供する可能性がある（McCabe, et al., 2012; Knutson, et al., 2014; Brach, et al., 2017）。

* 変異アミノ酸残基の位置は GenBank データベース *EZH2* NM_004456.3 に基づく。

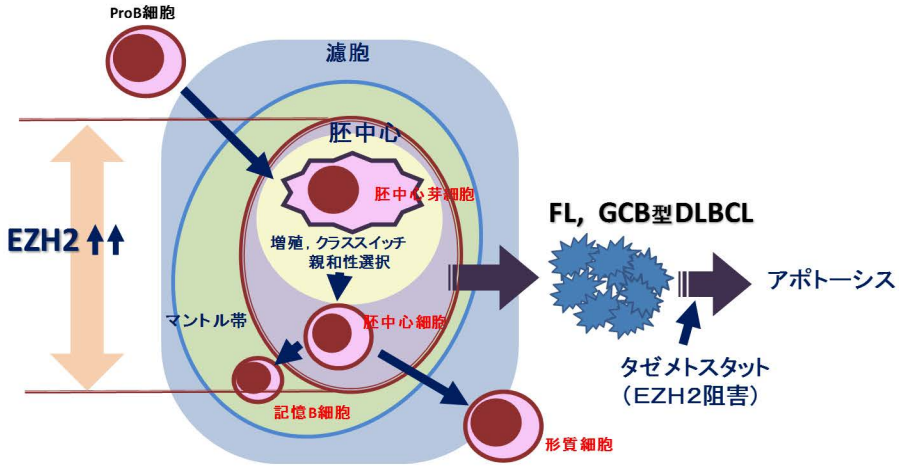


図 2.6.2.6-1　FL 及び GCB 型 DLBCL の起原と EZH2 発現

DLBCL = びまん性大細胞型 B 細胞性リンパ腫，FL = 濾胞性リンパ腫，GCB = 胚中心 B 細胞様.

ヒト FL で *EZH2* 変異を有する細胞株は知られていない。一方，GCB 型 DLBCL では *EZH2* 変異を有する細胞株として WSU-DLCL2，KARPAS-422，Pfeiffer，RL，SU-DHL-10，SU-DHL-6 等，また *EZH2* が野生型の細胞株として OCI-Ly19，Toledo，MC116 等が知られている。上述のように，FL と GCB 型 DLBCL は，ともに胚中心芽細胞及び胚中心細胞を由来とし，EZH2 を含む各種クロマチン修飾酵素遺伝子の異常，BCL2 の高発現や PI3K シグナルの亢進など一定の共通し

た分子生物学的な性状を有している（Alizadeh, et al., 2000; van Besien and Schouten, 2007; Pon and Marria, 2016; Green, 2018）。このことから，タゼメトスタットの非臨床薬理試験（in vitro 及び in vivo 試験）においては，B 細胞性リンパ腫として各種ヒト GCB 型 DLBCL の細胞株を用いた。

EZH2 をサブユニットとして含むポリコーム抑制複合体 PRC2 の他，SWI/SNF 複合体もヒストンの翻訳後修飾に重要な役割を担っており，PRC2 と SWI/SNF 複合体は多くの場合互いに拮抗的に働く。がんの約 20%で SWI/SNF 複合体のサブユニットである INI1（別名 SNF5，SMARCB1），SMARCA2，SMARCA4，ADRID1A，PBRM1 等の遺伝子変異や欠損が認められている（Kadoch and Crabtree, 2013; Kadoch, et al., 2016）。この内，*INI1* 欠損悪性ラブドイド腫瘍では，INI1 の欠損に起因する SWI/SNF 複合体の機能異常が生じ，SWI/SNF 複合体と PRC2 の不均衡により EZH2 の活性抑制が解除される（Wilson, et al., 2010）。滑膜肉腫では遺伝子転座による融合タンパク質 SS18-SSX1/2 形成のため INI1 がタンパク質として不安定化しており，これも EZH2 の活性抑制の解除につながる。これは SWI/SNF 複合体において，SS18 の替わりに SS18-SSX1/2 が組み込まれることによって，INI1 が SWI/SNF 複合体から追い出され，タンパク質分解酵素による分解を受けやすくなるためである（Kadoch and Crabtree, 2013）。SCCOHT では *SMARCA2* 及び *SMARCA4* が二重に欠損しており，これにともない EZH2 に依存した細胞増殖をおこす（Jelinic, et al., 2016; Chan-Penebre, et al., 2017）。このように，*EZH2* 変異のみならず，SWI/SNF 複合体の各種サブユニットの異常（*INI1* 欠損，*SS18-SSX1/2* 融合，*SMARCA2/4* 二重欠損等）によっても EZH2 の活性抑制の解除がおき，がん腫によってはこれに EZH2 以外のクロマチン修飾酵素の変異等も影響して H3K27me3 レベルが亢進し，がん発症及び悪性化に至ると考えられる。タゼメトスタットの非臨床薬理試験（in vitro 試験）においては，*INI1* 欠損あるいは *SS18-SSX1/2* 融合が生じている各種悪性軟部腫瘍，*SMARCA2/4* 二重欠損が生じている SCCOHT の各種細胞株を用いた。

タゼメトスタットは無細胞系において，野生型及び変異型 EZH2 の酵素活性を IC_{50} 値 2～38 nmol/L で阻害した。野生型及び変異型 EZH2 に対する阻害は EZH2 と最も類縁の HMT である EZH1 に対する阻害と比較して 36 倍，またその他の HMT に対する阻害と比較して 3000 倍以上強く，本薬は EZH2 に対する特異的阻害剤であることが示された。EZH2 に対する阻害の IC_{50} 値はメチル基のドナー基質である SAM の濃度に応じて増加したが，オリゴヌクレオソーム濃度を変えてもほとんど変化しないことから，本薬による阻害が SAM 競合的であることが示唆された。タゼメトスタットは DLBCL 細胞株のヒストンにおいて特異的にメチル化 H3K27 のレベルを低下させたことより，細胞系においても EZH2 を特異的に阻害することが示唆された。

タゼメトスタットは *EZH2* 変異を有する各種ヒト DLBCL 細胞株の細胞増殖を強力に阻害し，IC_{50} 値は計 6 株の内 5 株に対し，10^{-10}～10^{-9} モルオーダーであった。次いで，*INI1* が欠損あるいは INI1 がタンパク質として不安定化したヒト悪性軟部腫瘍細胞 6 株，*SMARCA2* 及び *SMARCA4* をともに欠損しているヒト SCCOHT 細胞 4 株に対し，10^{-8}～10^{-7} モルオーダーの IC_{50} 値を示した。*EZH2* 野生型のヒト DLBCL 細胞 4 株の細胞増殖に対しても 10^{-7}～10^{-6} モルオーダーの IC_{50} 値を示した。対照とした *INI1*[+]あるいは INI1 正常の細胞 4 株に対する IC_{50} 値は 10^{-6} モル以上であった。以上本薬は *EZH2* 変異ないし EZH2 活性が亢進していると考えられるがん細胞株に対し強

い細胞増殖阻害を示した。細胞増殖阻害の機序は，細胞周期の G1 期停止とそれに続くアポトーシス誘導であり，G1 期停止の時期（培養 4 日～7 日）は細胞内 H3K27me3 が消失する時期と対応していた。

EZH2 変異を有するヒト DLBCL 細胞株（WSU-DLCL2，KARPAS-422，Pfeiffer 及び SU-DHL-10）を用いたマウス移植モデルにおいて，タゼメトスタットの 1 日 2 回あるいは 3 回，28 日等の経口投与は 34.2 から 532 mg/kg の範囲の用量において TGI から腫瘍縮小に至る有意な抗腫瘍効果を示した。腫瘍組織の H3K27me3 レベルは本薬の用量及び時間依存的に低下したことから，本薬の抗腫瘍効果が EZH2 阻害に基づくことが示唆された。*EZH2* が野生型であるヒト DLBCL 細胞株（OCI-Ly19，Toledo 及び MC116）を用いたマウス移植モデルにおいて，タゼメトスタット（571 mg/kg）の 1 日 2 回，17～28 日間の経口投与は，腫瘍縮小は示さないものの有意な TGI を示した。このことは本薬が in vitro において，*EZH2* が野生型であるヒト DLBCL 細胞株に対しても，*EZH2* 変異を有するヒト DLBCL 細胞株より弱いながら細胞増殖阻害作用を示したことと対応していた。*EZH2* 変異を有するヒト DLBCL 細胞株（WSU-DLCL2 及び SU-DHL-10）移植モデルにおいて，タゼメトスタットと DLBCL の治療に使用される化学療法レジメンとの併用（ドキソルビシン併用の有りと無しを含む）は，それぞれの単独投与より優れた抗腫瘍効果を発揮した。以上の各種ヒト腫瘍移植モデルにおいて，タゼメトスタット単独の投与群で BWL はほとんどない，あるいは 10%以下であった。

以上の結果より，タゼメトスタットは各種ヒト DLBCL 細胞株移植モデルにおいて，顕著な BWL を伴わずに TGI から腫瘍縮小に至る抗腫瘍効果を発揮し，これは本薬の EZH2 阻害による腫瘍細胞内 H3K27me3 レベルの低下によるものと考えられた。以上の非臨床薬理成績は，タゼメトスタットが，FL など EZH2 に依存性のある腫瘍に対して有効な治療法となる可能性を支持した。

各種受容体，トランスポーター及びイオンチャネルからなる 80 種の分子パネルのリガンド結合に対するタゼメトスタット（10 μmol/L）の作用を標識リガンド結合アッセイで検討した。その結果，79 種の各種受容体，トランスポーター及びイオンチャネルにおいて，各々のリガンド結合に対する 50%を超える阻害あるいは促進は認められなかった。タゼメトスタットはムスカリン性アセチルコリン受容体 M4 とそのリガンドとの結合を IC_{50} 値 4.6 μmol/L で阻害したが，同受容体の細胞機能アッセイではアゴニスト作用，アンタゴニスト作用のいずれも示さなかった。また，タゼメトスタット（10 μmol/L）は 40 種類のヒトキナーゼ（セリン・スレオニンキナーゼ及びチロシンキナーゼを含むパネルにおいて，いずれの酵素活性に対しても有意な阻害を示さなかった。

タゼメトスタットは，ラット及びカニクイザルの PBMCs，骨髄，脾臓及び皮膚における H3K27me3 レベルを用量依存的に低下させ，その作用は特に骨髄で最も強力であった。ラット皮膚における H3K27me3 レベルの低下は 1 日 1 回 7 日間投与では観測されず，1 日 1 回 22～28 日間投与で有意に阻害された。

心血管系に及ぼす影響については，hERG を発現させた HEK293 細胞を用いた電気生理学的 in vitro 試験，ウサギ左心室ウェッジ標本を用いた電気生理学的 ex vivo 試験及びテレメトリー送信器を埋め込んだ覚醒サルを用いた単回経口投与試験を実施した。中枢神経系及び呼吸器系に及ぼす影響については，サルを用いた 28 日間反復経口投与毒性試験に組み込んで神経学的機能検査及び呼吸機能測定を実施した。

タゼメトスタットの 10 μmol/L は hERG チャネル発現細胞における hERG カリウム電流を 15.1%阻害した。ウサギ左心室ウェッジ標本において，タゼメトスタットの 20 μmol/L まで QRS 時間には影響しなかったが，20 μmol/L で QT 間隔は短縮し，7 及び 20 μmol/L で $T_{p\text{-}e}$ 間隔は短縮した。しかし，どの濃度でも不整脈性事象の発生は認められなかった。覚醒サルにおいて，最高投与量の 1000 mg/kg（臭化水素酸塩として）まで心血管パラメータ（心拍数，平均血圧及び心電図）への影響は認められなかった。サル反復経口投与毒性試験の第 7 日に実施された神経学的機能検査において，タゼメトスタットの 300 mg/kg（臭化水素酸塩として）まで影響は認められず，最高用量の 1000 mg/kg（臭化水素酸塩として）では両側後肢の筋緊張低下がみられたが，これは一般状態悪化の影響と考えられた。サル反復経口投与毒性試験の第 6 日に実施された呼吸機能測定において，最高投与量の 1000 mg/kg（臭化水素酸塩として）まで呼吸機能（呼吸数及び 1 回換気量）への影響はみられなかった。

これらの結果から，心血管系，中枢神経系及び呼吸器系のリスクは認められなかった。

2.6.2.7 図表

薬理試験の概要文中の図表は，本文中の適切な箇所に記載した。

2.6.2.8 参考文献

Alimova I, Birks DK, Harris PS, Knipstein JA, Venkataraman S, Marquez VE, et al. Inhibition of EZH2 suppresses self-renewal and induces radiation sensitivity in atypical rhabdoid teratoid tumor cells. Neuro-oncology. 2013;15:149–60.

Alizadeh AA, Eisen MB, Davis RE, Ma C, Lossos IS, Rosenwald A, et al. Distinct types of diffuse large B-cell lymphoma identified by gene expression profiling. Nature. 2000;403:503–11.

Arisan S, Buyuktuncer ED, Palavan-Unsal N, Çaşkurlu T, Çakir OO, Ergenekon E. Increased expression of EZH2, a polycomb group protein, in bladder carcinoma. Urologia Internationalis. 2005;75:252–7.

Beguelin W, Popovic R, Teater M, Jiang Y, Bunting KL, Rosen M, et al. EZH2 is required for germinal center formation and somatic EZH2 mutations promote lymphoid transformation. Cancer Cell. 2013;23:677–92.

Beguelin W, Teater M, Gearhart MD, Calvo Fernández MT, Goldstein RL, Cárdenas MG, et al. EZH2 and BCL6 cooperate to assemble CBX8-BCOR complex to repress bivalent promoters, mediate germinal center formation and lymphomagenesis. Cancer cell. 2016;30:197–213.

Bödör C, Grossmann V, Popov N, Okosun J, O'riain C, Tan K, et al. EZH2 mutations are frequent and represent an early event in follicular lymphoma. Blood. 2013;122:3165–8.

Brach D, Johnston-Blackwell D, Drew A, Lingaraj T, Motwani V, Warholic NM, et al. EZH2 inhibition by tazemetostat results in altered dependency on B-cell activation signaling in DLBCL. Molecular Cancer Therapeutics. 2017;16:2586–97.

Caganova M, Carrisi C, Varano G, Mainoldi F, Zanardi F, Germain P-L, et al. Germinal center dysregulation by histone methyltransferase EZH2 promotes lymphomagenesis. The Journal of clinical investigation. 2013;123:5009–22.

Chan-Penebre E, Armstrong K, Drew A, Grassian AR, Feldman I, Knutson SK, et al. Selective killing of SMARCA2- and SMARCA4-deficient small cell carcinoma of the ovary, hypercalcemic type cells by inhibition of EZH2: in vitro and in vivo preclinical models. Molecular Cancer Therapeutics. 2017;16:850–60.

Chase A, Cross NCP. Aberrations of EZH2 in cancer. Clinical Cancer Research. 2011;17:2613–8.

Copeland RA. Molecular pathways: protein methyltransferases in cancer. Clinical Cancer Research. 2013;19:6344–50.

Ennishi D, Takata K, Béguelin W, Duns G, Mottok A, Farinha P, et al. Molecular and genetic characterization of MHC deficiency identifies EZH2 as therapeutic target for enhancing immune recognition. Cancer Discovery. 2019;9:546–63.

Green MR. Chromatin modifying gene mutations in follicular lymphoma. Blood. 2018;131:595–604.

Jelinic P, Schlappe BA, Conlon N, Tseng J, Olvera N, Dao F, et al. Concomitant loss of SMARCA2 and SMARCA4 expression in small cell carcinoma of the ovary, hypercalcemic type. Modern pathology. 2016;29:60–6.

Kadoch C, Crabtree GR. Reversible disruption of mSWI/SNF (BAF) complexes by the SS18-SSX oncogenic fusion in synovial sarcoma. Cell. 2013;153:71–85.

Kadoch C, Copeland RA, Keilhack H. PRC2 and SWI/SNF chromatin remodeling complexes in health and disease. Biochemistry. 2016;55:1600-14.

Kawano S, Grassian AR, Tsuda M, Knutson SK, Warholic NM, Kuznetsov G, et al. Preclinical evidence of

anti-tumor activity induced by EZH2 inhibition in human models of synovial sarcoma. PLoS One. 2016;11:e0158888.

Kim KH, Roberts CW. Targeting EZH2 in cancer. Nat Med. 2016;22:128–34.

Knutson SK, Warholic NM, Wigle TJ, Klaus CR, Allain CJ, Raimondi A, et al. Durable tumor regression in genetically altered malignant rhabdoid tumors by inhibition of methyltransferase EZH2. Proceedings of the National Academy of Sciences of the United States of America. 2013;110:7922–7.

Knutson SK, Kawano S, Minoshima Y, Warholic NM, Huang K-C, Xiao Y, et al. Selective inhibition of EZH2 by EPZ-6438 leads to potent antitumor activity in EZH2-mutant non-Hodgkin lymphoma. Molecular Cancer Therapeutics. 2014;13:842–54.

Margueron R, Reinberg D. The Polycomb complex PRC2 and its mark in life. Nature. 2011;469:343–9.

McCabe MT, Ott HM, Ganji G, Korenchuk S, Thompson C, Van Aller GS, et al. EZH2 inhibition as a therapeutic strategy for lymphoma with EZH2-activating mutations. Nature. 2012;492:108–12.

Mlynarczyk C, Fontán L, Melnick A. Germinal center-derived lymphomas: The darkest side of humoral immunity. Immunological reviews. 2019;288:214–39.

Morin RD, Johnson NA, Severson TM, Mungall AJ, An J, Goya R, et al. Somatic mutations altering EZH2 (Tyr641) in follicular and diffuse large B-cell lymphomas of germinal-center origin. Nature genetics. 2010;42:181–5.

Pon JR, Marra MA. Clinical impact of molecular features in diffuse large B-cell lymphoma and follicular lymphoma. Blood. 2016;127:181–6.

Shen JK, Cote GM, Gao Y, Choy E, Mankin HJ, Hornicek FJ, et al. Targeting EZH2-mediated methylation of H3K27 inhibits proliferation and migration of synovial sarcoma in vitro. Scientific Reports. 2016;6:25239.

Sneeringer CJ, Scott MP, Kuntz KW, Knutson SK, Pollock RM, Richon VM, et al. Coordinated activities of wild-type plus mutant EZH2 drive tumor-associated hypertrimethylation of lysine 27 on histone H3 (H3K27) in human B-cell lymphomas. Proceedings of the National Academy of Sciences of the United States of America. 2010;107:20980–5.

Van Besien K, Schouten H. Follicular lymphoma: a historical overview. Leukemia & Lymphoma. 2007;48:232–43.

Varambally S, Dhanasekaran SM, Zhou M, Barrette TR, Kumar-Sinha C, Sanda MG, et al. The polycomb group protein EZH2 is involved in progression of prostate cancer. Nature. 2002;419:624–9.

Velichutina I, Shaknovich R, Geng H, Johnson NA, Gascoyne RD, Melnick AM, et al. EZH2-mediated epigenetic silencing in germinal center B cells contributes to proliferation and lymphomagenesis. Blood. 2010;116:5247–55.

Wilson BG, Wang X, Shen X, Mckenna ES, Lemieux ME, Cho YJ, et al. Epigenetic antagonism between polycomb and SWI/SNF complexes during oncogenic transformation. Cancer Cell. 2010;18:316–28.

Yap DB, Chu J, Berg T, Schapira M, Cheng SWG, Moradian A, et al. Somatic mutations at EZH2 Y641 act dominantly through a mechanism of selectively altered PRC2 catalytic activity, to increase H3K27 trimethylation. Blood. 2011;117:2451–9.

Yoo KH, Hennighausen L. EZH2 methyltransferase and H3K27 methylation in breast cancer. International journal of biological sciences. 2012;8:59–65.

Zingg D, Debbache J, Schaefer SM, Tuncer E, Frommel SC, Cheng P, et al. The epigenetic modifier EZH2 controls melanoma growth and metastasis through silencing of distinct tumour suppressors. Nat Commun. 2015;6:6051.

目次

2.6.3 薬理試験概要表 2
2.6.3.1 薬理試験：一覧表 2
2.6.3.2 効力を裏付ける試験 6
2.6.3.3 副次的薬理試験 13
2.6.3.4 安全性薬理試験 14
2.6.3.5 薬力学的薬物相互作用試験 16

2.6.3 薬理試験概要表

2.6.3.1 薬理試験：一覧表

被験物質：タゼメトスタット

Type of Study	Test System	Method of Administration	Testing Facility	Study Number	CTD Location
効力を裏付ける試験					
Inhibition of cell free HMT activity	Human/ A panel of recombinant HMTs cell free enzyme assay	in vitro	[redacted]	E7438-PD006	4.2.1.1.1
Inhibition of cellular HMT activity	Human/WSU-DLCL2 (DLBCL) histone methylation assay	in vitro	[redacted]	E7438-PD007	4.2.1.1.2
Inhibition of cell proliferation, cellular HMT activity, and mechanism of cell killing	Human/ A panel of lymphoma cell lines cell proliferation assay, histone methylation assay, cell cycle analysis, apoptosis assay	in vitro	[redacted]	E7438-PD009	4.2.1.1.3
Inhibition of cell free and cellular HMT activity by tazemetostat metabolites	Human/ Recombinant EZH2 cell free enzyme assay WSU-DLCL2 (DLBCL) histone methylation assay	in vitro	[redacted]	E7438-PD018	4.2.1.1.4
Inhibition of cell proliferation	Human/ WSU-DLCL2 (DLBCL) cell proliferation assay	in vitro	[redacted]	E7438-PD008	4.2.1.1.5
EZH2 mutation analysis	Human/ A panel of lymphoma cell lines Sanger sequencing of genomic DNA	in vitro	[redacted]	E7438-PD010	4.2.1.1.6

被験物質：タゼメトスタット

Type of Study	Test System	Method of Administration	Testing Facility	Study Number	CTD Location
Inhibition of cell proliferation, cellular HMT activity, and mechanism of cell killing	Human/ A panel of MRT, rhabdomyosarcoma and embryonic kidney cell lines histone methylation assay; cell proliferation assay; cell cycle analysis; apoptosis assay	in vitro	[redacted]	E7438-PD011	4.2.1.1.7
Inhibition of cell proliferation	Human/ A panel of synovial sarcoma cell lines cell proliferation assay	in vitro	Eisai Co., Ltd	M[redacted]023	4.2.1.1.8
Inhibition of cell proliferation, cellular HMT activity, and mechanism of cell killing	Human/ A panel of SCCOHT cell lines histone methylation assay; cell proliferation assay; apoptosis assay	in vitro	[redacted]	E7438-PD026	4.2.1.1.9
Effects on tumor growth and H3K27 methylation in human cancer xenograft model in mice	Mouse/SCID, Human/WSU-DLCL2 (DLBCL) xenograft model	PO	[redacted]	E7438-PD001	4.2.1.1.10
Effects on tumor growth in human cancer xenograft model in mice	Mouse/BALB/c-nu, Human/KARPAS-422 (DLBCL) xenograft model	PO	Eisai Co., Ltd	M[redacted]024	4.2.1.1.11
Effects on tumor growth in human cancer xenograft model in mice	Mouse/BALB/c-nu, Human/KARPAS-422 (DLBCL) xenograft model	PO	Eisai Co., Ltd	M[redacted]002	4.2.1.1.12
Effects on H3K27 methylation in human cancer xenograft model in mice	Mouse/BALB/c-nu, Human/KARPAS-422 (DLBCL) xenograft model	PO	Eisai Co., Ltd	W-20[redacted]0483	4.2.1.1.13

被験物質：タゼメトスタット

Type of Study	Test System	Method of Administration	Testing Facility	Study Number	CTD Location
Effects on tumor growth in human cancer xenograft model in mice	Mouse/NOD-SCIDγ, Human/Pfeiffer (DLBCL) xenograft model	PO	Eisai Inc.	PPC20[redacted]-03N	4.2.1.1.14
Effects on tumor growth in human cancer xenograft model in mice	Mouse/SCID, Human/OCI-Ly19 (DLBCL) xenograft model	PO	[redacted]	CPB-P[redacted]-5184-OCI-Ly19	4.2.1.1.15
Effects on tumor growth in human cancer xenograft model in mice	Mouse/SCID, Human/Toledo (DLBCL) xenograft model	PO	[redacted]	CPB-P[redacted]-5184-Toledo	4.2.1.1.16
Effects on tumor growth in human cancer xenograft model in mice	Mouse/SCID, Human/MC116 (DLBCL) xenograft model	PO	[redacted]	CPB-P[redacted]-5184-MC116	4.2.1.1.17
Effects on tumor growth and H3K27 methylation in human cancer xenograft model in mice	Mouse/SCID, Human/SU-DHL-10 (DLBCL) xenograft model	PO	[redacted]	E7438-PD002	4.2.1.1.18
副次的薬理試験					
Effects on a panel of 80 cellular targets (receptors, channels, and transporters)	High-throughput profile study (ExpressProfile) using a panel of cellular targets except for kinases Ligand binding assay, cAMP assay	in vitro	[redacted]	864269-864279-864288	4.2.1.2.1
Effects on a panel of 40 kinases (serine/threonine and tyrosine kinases)	A panel of recombinant kinases (40 enzymes containing both serine/threonine and tyrosine kinases) cell free enzyme assay	in vitro	[redacted]	EPI001	4.2.1.2.2

被験物質：タゼメトスタット

Type of Study	Test System	Method of Administration	Testing Facility	Study Number	CTD Location
Effects on H3K27 methylation in Sprague Dawley rats (7 days treatment)	Rat/Sprague Dawley histone methylation assay	PO	[redacted]	E7438-PD003	4.2.1.2.3
Effects on H3K27 methylation in Sprague Dawley rats (28 days treatment)	Rat/Sprague Dawley histone methylation assay	PO	[redacted]	E7438-PD004	4.2.1.2.4
Effects on H3K27 methylation in cynomolgus monkeys	Monkey/cynomolgus histone methylation assay	PO	[redacted]	E7438-PD005	4.2.1.2.5
安全性薬理試験					
hERG potassium channels expressed in mammalian cells	HEK293 cells transfected with hERG	In vitro	[redacted]	[redacted]0517.FQJ	4.2.1.3.1
QT, QRS, T_{p-e} and arrhythmogenesis in the rabbit left ventricular wedge preparation	Rabbit	Ex vivo	[redacted]	LIMR-20[redacted]0801	4.2.1.3.2
CV safety pharmacology assessment in telemetered cynomolgus monkeys	Monkey/cynomolgus	PO	[redacted]	20026297	4.2.1.3.3
CNS assessment in cynomolgus monkey (4-week toxicity study)	Monkey/cynomolgus	PO	[redacted]	20024293	4.2.3.2.5
Respiratory system assessment in cynomolgus monkey (4-week toxicity study)	Monkey/cynomolgus	PO	[redacted]	20024293	4.2.3.2.5

cAMP = cyclic adenosine monophosphate; CNS = central nervous system; CTD = Common Technical Document, CV = cardiovascular; ECG = electrocardiogram; H3K27 = lysine 27 of histone H3, HEK = human embryonic kidney, hERG = human ether-à-go-go-related gene, HMT = histone methyltransferase, IC_{50} = 50% inhibitory concentration, NA = not applicable, PO = oral, SAM = S-adenosylmethionine, SCCOHT = small cell carcinoma of the ovary hypercalcemic type, T_{p-e} = interval between the end and the peak of T wave.

2.6.3.2 効力を裏付ける試験

被験物質：タゼメトスタット

Type of Study	Methods	Species/Strain	Route	Dose or Concentration	Observations	Study No. (CTD Location)
Inhibition of cell free HMT activity	Measurement of SAM derived radiolabeled methyl group incorporation into avian erythrocyte oligonucleosomes or histone derived peptide substrates.	Human/recombinant PRC2 containing EZH2, EZH1, or EZH2 with mutations, a panel of other recombinant HMTs	In vitro	Tazemetostat HCl, HBr, or free form: 10,000 nmol/L (determination of percent inhibition) 0.025-500 nmol/L for EZH2 130-2,500,000 nmol/L for other HMTs (determination of IC_{50})	Tazemetostat inhibited wild-type EZH2 with an IC_{50} value of 11 ± 5 nmol/L (using histone derived peptide substrate containing H3K27), showing 36-fold selectivity over the closest family member EZH1, and greater than 3000-fold selectivity over the other HMTs. Tazemetostat inhibited mutant-type EZH2s with IC_{50} values ranging from 2 to 38 nmol/L.	E7438-PD006 (4.2.1.1.1)
Inhibition of cellular HMT activity	ELISA or western blotting of histones extracted from cells using antibodies specific for H3K27me1, H3K27me2, H3K27me3, H3K27acetyl, H3K4me3, H3K9me3, H3K36me2, H3K79me2, or total H3.	Human/WSU-DLCL 2 (DLBCL, *EZH2* mutant), OCI-Ly19 (DLBCL, *EZH2* wild type)	In vitro	Tazemetostat HCl or HBr: 0.13-25,000 nmol/L (ELISA, determination of IC_{50}) Tazemetostat HCl: 1000 nmol/L (western blot) Tazemetostat (salt forms were not recorded): 2700 nmol/L (western blot)	Tazemetostat inhibited intracellular H3K27 methylation in a concentration-dependent manner (IC_{50} value = 0.26 μmol/L) and time-dependent manner in *EZH2* mutant-type lymphoma cells. Tazemetostat selectively inhibited intracellular H3K27 methylation in *EZH2* wild-type lymphoma cells.	E7438-PD007 (4.2.1.1.2) E7438-PD009 (4.2.1.1.3)

被験物質：タゼメトスタット

Type of Study	Methods	Species/Strain	Route	Dose or Concentration	Observations	Study No. (CTD Location)
Inhibition of cell free HMT activity by tazemetostat metabolites	Measurement of SAM derived radiolabeled methyl group incorporation into histone derived peptide substrate containing H3K27.	Human/recombinant PRC2 containing EZH2	In vitro	Tazemetostat metabolites	Tazemetostat metabolites inhibited wild-type EZH2 with IC_{50} values in the 3 nmol/L to 6 μmol/L range. EPZ-6930 (major metabolite) with IC_{50} value of 120 ± 30 nmol/L is at least 11-fold less potent than tazemetostat.	E7438-PD018 (4.2.1.1.4)
Inhibition of cell proliferation	Quantification of viable cell number by measuring depletion of metabolic ATP (6-day proliferation assay).	Human/WSU-DLCL2 (*EZH2* mutant)	In vitro	Tazemetostat HCl: 3.0-20,000 nmol/L (6 days)	Tazemetostat selectively inhibited the proliferation of *EZH2* mutant lymphoma cells with an average IC_{50} value of 0.28 ± 0.14 μmol/L.	E7438-PD008 (4.2.1.1.5)
Inhibition of cell proliferation and mechanism of cell killing	Quantification of viable cell number by measuring depletion of metabolic ATP (6-day proliferation assay), or direct viable cell counting (11- or 14-day proliferation assay). Measurement of effect on cell cycle by flow cytometry for DNA content. Measurement of apoptosis by flow cytometry for DNA content and TUNEL assay.	Human/a panel of lymphoma cell lines with either wild-type or mutant *EZH2*	In vitro	Tazemetostat HCl or free form [a]: 0.0024-25,000 nmol/L (11 or 14 days) Tazemetostat HCl: 1000 nmol/L (cell cycle analysis, TUNEL)	Tazemetostat selectively inhibited the proliferation of *EZH2* mutant lymphoma cells with IC_{50} values from 0.49 to 8.6 nmol/L except for RL cells. Tazemetostat selectively inhibited the proliferation of *EZH2* wild-type lymphoma cells with IC_{50} values from 99 to 7600 nmol/L. Cell killing required more than 4 days of continuous exposure to tazemetostat. Cell death occurred via G1 cell cycle arrest by Day 4, followed by induction of apoptosis by Day 14 in WSU-DLCL2 cell lines.	E7438-PD009 (4.2.1.1.3)

被験物質：タゼメトスタット

Type of Study	Methods	Species/Strain	Route	Dose or Concentration	Observations	Study No. (CTD Location)
EZH2 mutation analysis	Sanger sequencing of genomic DNA from cell lines.	Human/a panel of lymphoma cell lines	In vitro	NA	Identification of *EZH2* mutations in a subset of human lymphoma cell lines.	E7438-PD010 (4.2.1.1.6)
Inhibition of histone methylation, inhibition of cell proliferation, and mechanism of cell killing	Histone methylation by quantitative immunoblot. Quantification of viable cell number by measuring depletion of metabolic ATP (14-day proliferation assay). Measurement of effect on cell cycle by flow cytometry for DNA content. Measurement of apoptosis by flow cytometry for DNA content and TUNEL assay.	Human/a panel of *INI1*-negative MRT cell lines and *INI1* positive cell lines (rhabdomyosarcoma and human embryonic kidney)	In vitro	Tazemetostat HBr: 0.006 to 1100 nmol/L (methylation) 0.6 to 10,000 nmol/L (proliferation) 1000 nmol/L (cell cycle analysis, TUNEL)	H3K27me3 was inhibited in all cells tested. Tazemetostat selectively inhibited the proliferation of *INI1*-negative MRT cells with IC_{50} values in the submicromolar range (0.032 to 1.0 μmol/L). Cell killing required more than 4 days of continuous exposure to tazemetostat. Cell death occurred via G1 cell cycle arrest by Day 4, followed by induction of apoptosis after Day 7.	E7438-PD011 (4.2.1.1.7)
Inhibition of cell proliferation	Quantification of viable cell number by measuring depletion of metabolic ATP (14-day proliferation assay).	Human/synovial sarcoma cell lines	In vitro	Tazemetostat HBr: 39 to 10,000 nmol/L	Tazemetostat selectively inhibited the proliferation of synovial sarcoma cells with *INI1* deficiency with IC_{50} values of 0.15 μmol/L (Fuji cells) and 0.52 μmol/L (HS-SY-II cells). Antiproliferative effects required more than 4 days of continuous exposure to tazemetostat.	M[redacted]023 (4.2.1.1.8)

被験物質：タゼメトスタット

Type of Study	Methods	Species/Strain	Route	Dose or Concentration	Observations	Study No. (CTD Location)
Inhibition of histone methylation, inhibition of cell proliferation	Histone methylation by quantitative immunoblot. Quantification of viable cell number by measuring depletion of metabolic ATP (14-day proliferation assay). Measurement of effect on cell cycle by flow cytometry for DNA content.	Human/a panel of *SMARCA2/4*-negative SCCOHT cell lines	In vitro	Tazemetostat HBr: 0.508 to 10,000 nmol/L	H3K27me3 was inhibited in all cells tested. Tazemetostat selectively inhibited the proliferation of *SMARCA2/4*-negative SCCOHT cells with IC_{50} values in the submicromolar range (0.073 to 0.86 μmol/L).	E7438-PD026 (4.2.1.1.9)
Effects on tumor growth and H3K27 methylation in human cancer xenograft model in mice (4-week treatment)	Xenograft generation by SC inoculation of the cancer cells. Tumor volume measurement every 3 or 4 days. Measurement of tazemetostat levels in plasma and tumor homogenates by LC-MS/MS. Analysis of H3K27 methylation in histones isolated from the tumors by ELISA using anti-H3K27me3 or anti-total H3 antibody.	Mouse/female SCID Human cell/ WSU-DLCL2 (DLBCL *EZH2* mutant)	PO	Tazemetostat HCl: 40, 80, 160 mg/kg TID for 28 days	Dose-dependent TGI with a dT/C value of 42% at the highest dose. Dose-dependent increase in plasma and tumor tissue exposure. Dose-dependent inhibition of H3K27 methylation in tumors.	E7438-PD001 (4.2.1.1.10)

被験物質：タゼメトスタット

Type of Study	Methods	Species/Strain	Route	Dose or Concentration	Observations	Study No. (CTD Location)
Effects on tumor growth in human cancer xenograft model in mice	Xenograft generation by SC inoculation of cancer cells Tumor volume measurement every 3 or 4 days.	Mouse/female BALB/c-nu Human cell/ KARPAS-422 (DLBCL *EZH2* mutant)	PO	Tazemetostat HCl: 80.5, 161, 322, 644 mg/kg BID for 28 days	Dose-dependent antitumor effects, TGI at 80.5 mg/kg and tumor regressions with doses at 161 and 322 mg/kg. 644 mg/kg was not tolerated.	M[redacted]024 (4.2.1.1.11)
Effects on tumor growth in human cancer xenograft model in mice	Xenograft generation by SC inoculation of cancer cells. Tumor volume measurement every 3 or 4 days.	Mouse/female BALB/c-nu Human cell/ KARPAS-422 (DLBCL *EZH2* mutant)	PO	Tazemetostat HBr: 90, 361 mg/kg BID for 28 days, 90 and 361 mg/kg BID with the 2 cycles of 7-day on/ 7-day off regimen. 90 and 361 mg/kg BID with the 21-day on/7-day off regimen	Dose-dependent antitumor effects at all dosing schedules, TGI at 90 mg/kg and tumor regression at 361 mg/kg.	M[redacted]002 (4.2.1.1.12)
Effects on H3K27 methylation in human cancer xenograft model in mice (7 days treatment)	Xenograft generation by SC inoculation of cancer cells. Analysis of H3K27 methylation in histones isolated from the tumors by ELISA using anti-H3K27me3 or anti-total H3 antibody.	Mouse/female BALB/c-nu Human cell/ KARPAS-422 (DLBCL *EZH2* mutant)	PO	Tazemetostat HBr: 75, 150, 301, and 602 mg/kg BID for 7 days 150, 301, 602, and 1203 mg/kg QD for 7 days	Dose-dependent inhibition of H3K27 methylation in tumors.	W-20[redacted]0483 (4.2.1.1.13)

被験物質：タゼメトスタット

Type of Study	Methods	Species/Strain	Route	Dose or Concentration	Observations	Study No. (CTD Location)
Effects on tumor growth in human cancer xenograft model in mice	Xenograft generation by SC inoculation of cancer cells. Tumor volume measurement every 3 or 4 days.	Mouse/female NOD-SCID gamma Human cell/ Pfeiffer (DLBCL *EZH2* mutant)	PO	Tazemetostat HBr: 34.2, 114, and 342 mg/kg QD for 28 days 1140 mg/kg QD for 12 days	Dose-dependent antitumor effects. TGI at 34.2 mg/kg QD and tumor regressions with doses ≥114 mg/kg QD. 1140 mg/kg QD was not tolerated.	PPC20[redacted]-03N (4.2.1.1.14)
Effects on tumor growth in human cancer xenograft model in mice	Xenograft generation by SC inoculation of cancer cells. Tumor volume measurement every 3 or 4 days.	Mouse/female SCID Human cell/ OCI-Ly19 (DLBCL *EZH2* wild-type)	PO	Tazemetostat HBr: 143, and 571 mg/kg BID for 20 days	Dose-dependent antitumor effects with dT/C values of 65% and 26% on Day 21 at doses of 143 and 571 mg/kg BID, respectively.	CPB-P[redacted]-5184-OCI-Ly19 (4.2.1.1.15)
Effects on tumor growth in human cancer xenograft model in mice	Xenograft generation by SC inoculation of cancer cells. Tumor volume measurement every 3 or 4 days.	Mouse/female SCID Human cell/ Toledo (DLBCL *EZH2* wild-type)	PO	Tazemetostat HBr: 143, and 571 mg/kg BID for 28 days	Tazemetostat exhibited antitumor effects with a dT/C value of 71% on Day 29 at 571 mg/kg BID.	CPB-P[redacted]-5184-Toledo (4.2.1.1.16)
Effects on tumor growth in human cancer xenograft model in mice	Xenograft generation by SC inoculation of cancer cells. Tumor volume measurement every 3 or 4 days.	Mouse/female SCID Human cell/ MC116 (DLBCL *EZH2* wild-type)	PO	Tazemetostat HBr: 143, and 571 mg/kg BID for 17 days	Tazemetostat exhibited antitumor effects with a dT/C value of 34% on Day 18 at 571 mg/kg BID.	CPB-P[redacted]-5184-MC116 (4.2.1.1.17)

被験物質：タゼメトスタット

Type of Study	Methods	Species/Strain	Route	Dose or Concentration	Observations	Study No. (CTD Location)
Effects on tumor growth and H3K27 methylation in human cancer xenograft model in mice (combination with CHOP[a])	Xenograft generation by SC inoculation of cancer cells. Tumor volume measurement every 3 or 4 days. Measurement of tazemetostat levels in plasma by LC-MS/MS. Analysis of H3K27 methylation in histones isolated from the tumors by ELISA using anti-H3K27me3 or anti-total H3 antibody.	Mouse/female SCID Human cell/ WSU-DLCL2 (DLBCL *EZH2* mutant)	PO	Tazemetostat HCl: 160 mg/kg TID for 28 days; 239 and 319 mg/kg BID for 28 days; 638 mg/kg QD for 28 days CHOP[b] Tazemetostat HCl: 239 mg/kg BID for 28 days and CHOP[b]	Tazemetostat as single agent exhibited antitumor effects with dT/C values of 29% and 43% on Day 29 at doses of 239 and 319 mg/kg BID. CHOP resulted in 55% dT/C. Combination benefit when tazemetostat was given with CHOP[b] (7% dT/C). Inhibition of H3K27 methylation in tumors in tazemetostat-dosed animals.	E7438-PD001 (4.2.1.1.10)
Effects on tumor growth and H3K27 methylation in human cancer xenograft model in mice (combination with COP[b])	Xenograft generation by SC inoculation of cancer cells. Tumor volume measurement every 3 or 4 days. Measurement of tazemetostat levels in plasma by LC-MS/MS. Analysis of H3K27 methylation by ELISA using anti-H3K27me3 or anti-total H3 antibody in histones isolated from the tumors.	Mouse/female SCID Human cell/ SU-DHL-10 (DLBCL *EZH2* mutant)	PO	Tazemetostat HBr: 133, 266, and 532 mg/kg BID for 28 days COP[c] Tazemetostat HBr: 266 mg/kg BID for 28 days and COP[c]	Dose-dependent TGD effect with tazemetostat. Combination effect (TGI and TGD) when tazemetostat was given with COP compared to tazemetostat or COP alone. Dose-dependent increase in plasma exposure. Dose-dependent inhibition of H3K27 methylation in tumors. Tumor regressions with doses ≥266 mg/kg.	E7438-PD002 (4.2.1.1.18)

All doses on a weight base of tazemetostat are expressed as those of salt form (HCl salt or HBr salt). TGI activity was shown using dT/C values (dT/C [%] = dT/dC, dT and dC are changes of tumor volume from Day 1 for control group and treatment group, respectively (except for dT/C for OCI-Ly19-, Toledo-, and MC116-xenograft studies, which used Day –1). ATP = adenosine triphosphate, BID = twice daily, DLBCL = diffuse large B-cell lymphoma, DNA = deoxyribonucleic acid; ELISA = enzyme-linked immunosorbent assay; H3 = histone H3; H3K27 = histone H3 lysine 27; H3K27me3 = trimethylated form histone H3 lysine 27, HMT = histone methyltransferase, IC_{50} = 50% inhibitory concentration, IHC = immunohistochemistry, IP = intraperitoneal, IV = intravenous, LC-MS/MS = liquid-chromatography tandem mass spectrometry, NA = not

applicable; PO = oral, QD = once daily; SC = subcutaneous; SCCOHT = small cell carcinoma of the ovary hypercalcemic type, SCID = severe combined immunodeficiency, TGD = tumor growth delay, TGI = tumor growth inhibition; TID = 3 times a day, TUNEL = terminal deoxynucleotidyl transferase-mediated 2'-deoxyuridine 5'-triphosphate nick end labeling.
a: Salt forms of tazemetostat were not recorded in some experiments.
b: Cyclophosphamide was administered QD on Days 1 and 22 at 30 mg/kg IP; doxorubicin was administered QD on Days 1 and 22 at 2.475 mg/kg IV; vincristine was administered QD on Days 1 and 22 at 0.375 mg/kg IV; and prednisone was administered QD on Days 1 through 5 and Days 22 through 26 at 0.15 mg/kg QD×5 PO.
c: Cyclophosphamide was administered QD on Days 1 and 22 at 30 mg/kg IP; vincristine was administered QD on Days 1 and 22 at 0.375 mg/kg IV; and prednisone was administered QD on Days 1 through 5 and Days 22 through 26 at 0.15 mg/kg QD×5 PO.

2.6.3.3 副次的薬理試験

被験物質：タゼメトスタット

Type of Study	Methods	Species /Strain	Route	Dose	Observations	Study No. (CTD Location)
Effects on a panel of 80 cellular targets (receptors, channels, and transporters)	Ligand binding assay and cAMP functional assay using a panel of cellular targets (except for receptor kinases).	NA	In vitro	Tazemetostat HCl: 10 μmol/L (ligand binding), 0.03 to 100 μmol/L (determination of IC_{50}), 0.0025 to 50 μmol/L (functional assay)	No significant (higher than 50%) inhibition nor stimulation to any receptor except for muscarinic acetylcholine M4 receptor (IC_{50}: 4.6 μmol/L). Functional assay showed no agonistic nor antagonistic effect on the receptor.	864269-864279-864288 (4.2.1.2.1)
Effects on a panel of 40 kinases (serine/threonine and tyrosine kinases)	Cell free kinase assay using a panel of 40 enzymes containing both serine/threonine and tyrosine kinases.	NA	In vitro	Tazemetostat HCl: 10 μmol/L	None of the kinases were significantly inhibited at a tazemetostat concentration of 10 μmol/L.	EPI001 (4.2.1.2.2)

被験物質：タゼメトスタット

Type of Study	Methods	Species /Strain	Route	Dose	Observations	Study No. (CTD Location)
Effects on H3K27 methylation in Sprague Dawley rats (7 days treatment)	Analysis of H3K27 methylation in fixed skin specimens by IHC using anti-H3K27me3 antibody, or in histones isolated from selected tissues by ELISA using anti-H3K27me3 or anti-total H3 antibody.	Rat/female, Sprague Dawley	PO	Tazemetostat HCl: 106 and 319 mg/kg QD for 7 days	Dose-dependent inhibition of H3K27 methylation in spleen, PBMCs, and bone marrow but not skin.	E7438-PD003 (4.2.1.2.3)
Effects on H3K27 methylation in Sprague Dawley rats (4 weeks treatment)	Analysis of H3K27 methylation in fixed skin specimens by IHC using anti-H3K27me3 antibody, or in histones isolated from selected tissues by ELISA using antiH3K27me3 or anti-total H3 antibody as exploratory endpoint in the GLP toxicology study.	Rat/male and female, Sprague Dawley	PO	Tazemetostat HBr: 100, 300, and 1000 mg/kg QD for 28 day 1000 mg/kg QD for 22 days	Dose-dependent inhibition of H3K27 methylation in PBMCs, bone marrow, and skin in dosed animals. Bone marrow showed highest degree of H3K27me3 inhibition.	E7438-PD004 (4.2.1.2.4)
Effects on H3K27 methylation in cynomolgus monkeys	Analysis of H3K27 methylation in fixed skin specimens by IHC using anti-H3K27me3 antibody, or in histones isolated from selected tissues by ELISA using anti-H3K27me3 or anti-total H3 antibody as exploratory endpoint in the GLP toxicology study.	Monkey/male and female cynomolgus	PO	Tazemetostat HBr: 50, 150, and 500 (300)[a] mg/kg BID for 28 days	Dose-dependent inhibition of H3K27 methylation in skin in dosed animals, modest effect in PBMCs. Bone marrow showed highest degree of H3K27me3 inhibition.	E7438-PD005 (4.2.1.2.5)

All doses on a weight base of tazemetostat are expressed as those of salt form (HCl salt or HBr salt).
BID = twice daily, cAMP = cyclic adenosine monophosphate, DLBCL = diffuse large B-cell lymphoma, ELISA = enzyme-linked immunosorbent assay, GLP = Good

Laboratory Practice, H3 = histone H3, H3K27 = histone H3 lysine 27; H3K27me3 = trimethylated form histone H3 lysine 27, HMT = histone methyltransferase; IC_{50} = half-maximal inhibitory concentration; IHC = immunohistochemistry, IP = intraperitoneal, IV = intravenous, NA = not applicable; NOD = non-obese diabetic, PMBCs = peripheral blood mononuclear cells, PO = oral, QD = once daily; SC = subcutaneous; SCCOHT = small cell carcinoma of the ovary hypercalcemic type, SCID = severe combined immunodeficiency, TGI = tumor growth inhibition; TID = 3 times a day, TUNEL = terminal deoxynucleotidyl transferase dUTP nick end labeling.
a: Doses decreased from 500 to 300 mg/kg as of Days 11 (females) or 12 (males) after a 2.5-day period without drug administration.

2.6.3.4 安全性薬理試験

被験物質：タゼメトスタット

Organ Systems Evaluated	**Species /Strain**	**Methods of Administration**	**Dose**	**Gender and n per Group**	**Noteworthy Findings**	**GLP[a]**	**Study No. (CTD Location)**
hERG tail current	HEK293 cells transfected with hERG	In vitro and patch clamp	10 μmol/L (tazemetostat HCl)	NA	15.1 ± 1.4% inhibition at 10 μmol/L.	No	[redacted]0517.FQJ (4.2.1.3.1)
Left ventricular wedge preparation	Rabbit	Ex vivo and electrophysiology	0.75, 2.0, 7, and 20 μmol/L (tazemetostat HCl)	6 either males/females	No proarrhythmic events were induced up to 20 μmol/L Estimated TdP score was decreased at 7 and 20 μmol/L QRS duration was not changed up to 20 μmol/L QT interval was shortened at 20 μmol/L $T_{p\text{-}e}$ was shortened at 7 and 20 μmol/L.	No	LIMR-20[redacted]0801 (4.2.1.3.2)
CV system	Monkey/ cynomolgus	PO	100, 300, and 1000 mg/kg dose escalation, single dose (tazemetostat HBr)	4 females	No tazemetostat-related change in heart rate, blood pressure or ECG parameters up to 1000 mg/kg.	Yes	20026297 (4.2.1.3.3)

被験物質：タゼメトスタット

Organ Systems Evaluated	Species /Strain	Methods of Administration	Dose	Gender and n per Group	Noteworthy Findings	GLP[a]	Study No. (CTD Location)
CNS	Monkey/ cynomolgus	PO	100, 300, and 1000 mg/kg/day for 28 days, on Day 7 (tazemetostat HBr)	4 males 4 females	Decrease in muscle tone in both legs of 2 of the males at 1000 mg/kg/day, likely due to the poor clinical condition of animals.	Yes	20024293 (4.2.3.2.5)
Respiratory system	Monkey/ cynomolgus	PO	100, 300, and 1000 mg/kg/day for 28 days, on Day 6-7 (tazemetostat HBr)	4 males 4 females	No effects observed at any dose level of tazemetostat.	Yes	20024293 (4.2.3.2.5)

All doses on a weight base of tazemetostat are expressed as those of tazemetostat HBr salt.
a: An entry of "Yes" indicates that the study includes a GLP compliance statement.
CNS = central nervous system, CV = cardiovascular, ECG = electrocardiogram, GLP = Good Laboratory Practice, HEK = human embryonic kidney, hERG = human ether-a-go-go-related gene, NA = not applicable, PO = oral, TdP = torsades de pointes, $T_{p\text{-}e}$ = interval between the end and the peak of T wave.

2.6.3.5 薬力学的薬物相互作用試験

該当なし